

Electronic Supplementary Material (ESI) for Analytical Methods

A new rhodamine-based chemosensor for turn-on fluorescent detection of Fe^{3+}

XiangHan, Dong-En Wang, Shen Chen, Longlong Zhang, Yadan Guo, Jinyi Wang*

College of Science, Northwest A&F University, Yangling, Shaanxi 712100, PR China

* Corresponding author. Tel.: +86 29 87082520; fax: +86 29 87082520.

E-mail address: jywang@nwsuaf.edu.cn (J. Wang).

SI 1. The calculation method for the quantum yields. The quantum yields for fluorescence were obtained by comparison of the integrated area of the corrected emission spectrum of the samples with that of a solution of rhodamine B standard (ϕ_F 0.69 in ethanol).^{S1} The quantum efficiency of the metal-free and metal-bound RH-Fe was measured by using a dilute sample in H₂O–CH₃CN (7:3 v/v). The quantum yields were calculated with the expression in equation (Eq. 1):

$$\phi_u = \frac{A_s}{A_u} * \frac{F_u}{F_s} * \frac{n u^2}{n s^2} * \phi_s \quad (\text{Eq. 1})$$

where ϕ is the quantum yield, subscript *s* stands for the reference and *u* for the sample, *A* is the absorbance at the excitation wavelength, *n* is the refractive index, and *F* is the emission integrated area.

Table S1. Fluorescence quantum yield of RH-Fe.

Series	Maximum absorption wavelength (nm)	Maximum absorption	Start (nm)	End (nm)	Integral area of discharge	Fluorescence quantum yield
Rhodamin B	547	0.022	547	675	30211.964	0.69
RH-Fe+Fe ³⁺	561	0.010	561	675	10851.316	0.24

SI 2. Study on the selectivity of RH-Fe.



Figure S1. Color responses of RH-Fe (20 μM) in the presence of various metal ions (200 μM).

SI 3. Study on the selectivity of RH-Fe by UV-visible absorption spectra.

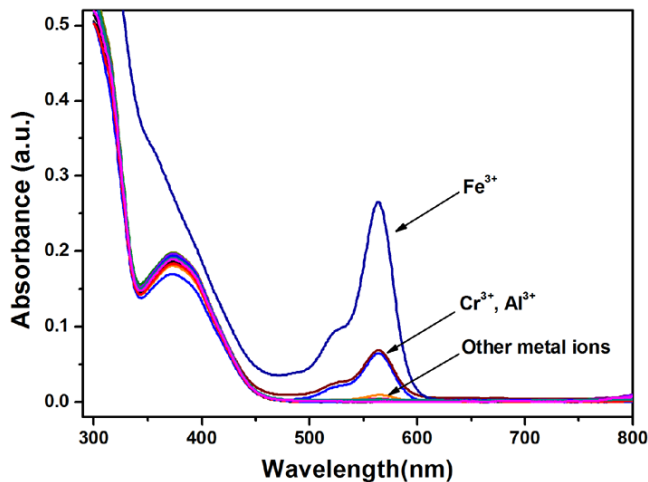


Figure S2. Absorbance spectra of RH-Fe (20 μM) in the presence of different metal ions (200 μM).

SI 4. The calculation method for the detection limit. The limit of detection (LOD) for RH-Fe was calculated based on the fluorescence titration.^{S1} To determine the S/N ratio, the emission intensity of RH-Fe without cations was measured by 10 times and the standard deviation of blank measurements was determined. Then, the linear range for Fe^{3+} was determined. The detection limit was calculated with the equation (Eq. 2) at $\text{S}/\text{N}=3$, in which σ is the standard deviation of the background and S is the sensitivity.

$$LOD = 3 \times \frac{\sigma}{S} \quad (\text{Eq. 2})$$

SI 5. The calculation method for the binding constant. The binding constant was determined using the Benesie-Hildebrand equation (Eq. 3):^{S2}

$$\frac{1}{I - I_0} = \frac{1}{K\alpha(I_{max} - I_0)[M^{x+}]^n} + \frac{1}{I_{max} - I_0} \quad (\text{Eq. 3})$$

where I is the measured fluorescence (absorption) intensity, I_{max} and I_0 are the signals with saturated cations and without cations, respectively, and $[M^{x+}]$ represent the concentrations of the cations.

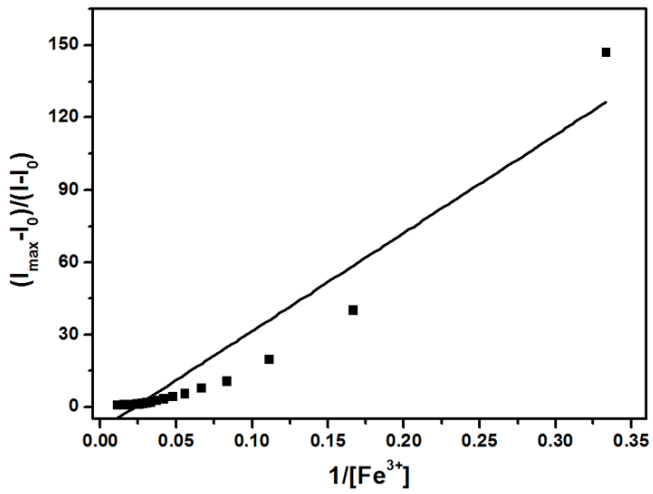
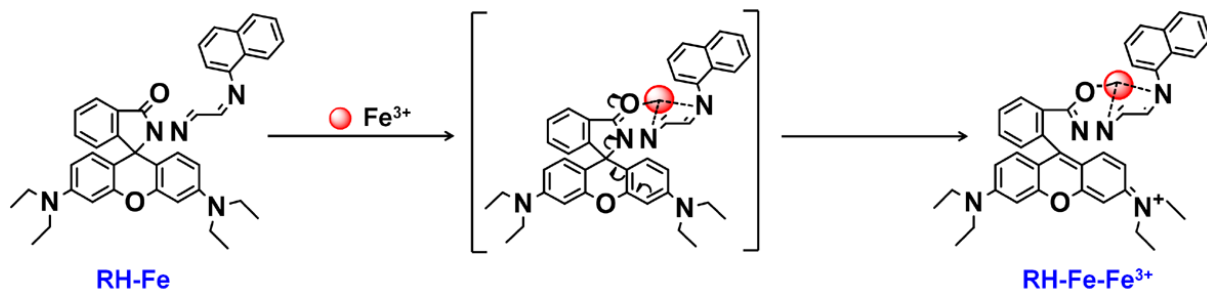


Figure S3. The relationship between $(I_{\max} - I_0)/(I - I_0)$ and $1/\text{[Fe}^{3+}]$.

SI 6. The mechanism of RH-Fe for Fe^{3+} detection.



Scheme S1. Proposed mechanism for the fluorescent changes of RH-Fe upon the addition of Fe^{3+} .

SI 7. Analysis of Fe^{3+} in real samples using probe RH-Fe.

Table S2. Analytical results for detection of Fe^{3+} in real samples.

Samples ^a	Fe ³⁺ spiked (μM)	Fe ³⁺ recovery (n=3) (μM)	Recovery (%)
Tap water	5	5.68 \pm 1.7	113.6
	10	7.73 \pm 2.4	77.3
	15	13.26 \pm 2.7	88.4
river water	5	5.64 \pm 0.05	112.8
	10	8.65 \pm 1.32	88.5
	15	13.39 \pm 1.22	89.3

^aThe sample contained 30% acetonitrile.

Table S3. Comparison of fluorescent probes for Fe³⁺

Probe	$\lambda_{\text{ex}}/\lambda_{\text{em}}$ (nm)	Detection medium	Detection limit	Ref
	520/582	CH ₃ CN:H ₂ O (95:5, v/v) solution	15 nM.	S3
	562/593	CH ₃ CN:H ₂ O (3:2, v/v) solution	1.8 μM.	S4
	530/550	THF:H ₂ O (99:1, v/v) solution	4.8 μM	S5
	260/345	DMSO:H ₂ O (50:50 v/v) solution	0.7 μM	S6
	315/498	DMSO:H ₂ O (1:1, v/v) solution	3.49 μM	S7
	550/585	CH ₃ OH:HEPES (1:1, v/v) solution	0.2 μM	S8
	558/580	CH ₃ OH solution	5 μM.	S9
	520/580	CH ₃ CN:H ₂ O (3:7, v/v) solution	0.27 μM	This work

S8. NMR spectra of Compound 1, 2, and RH-Fe.

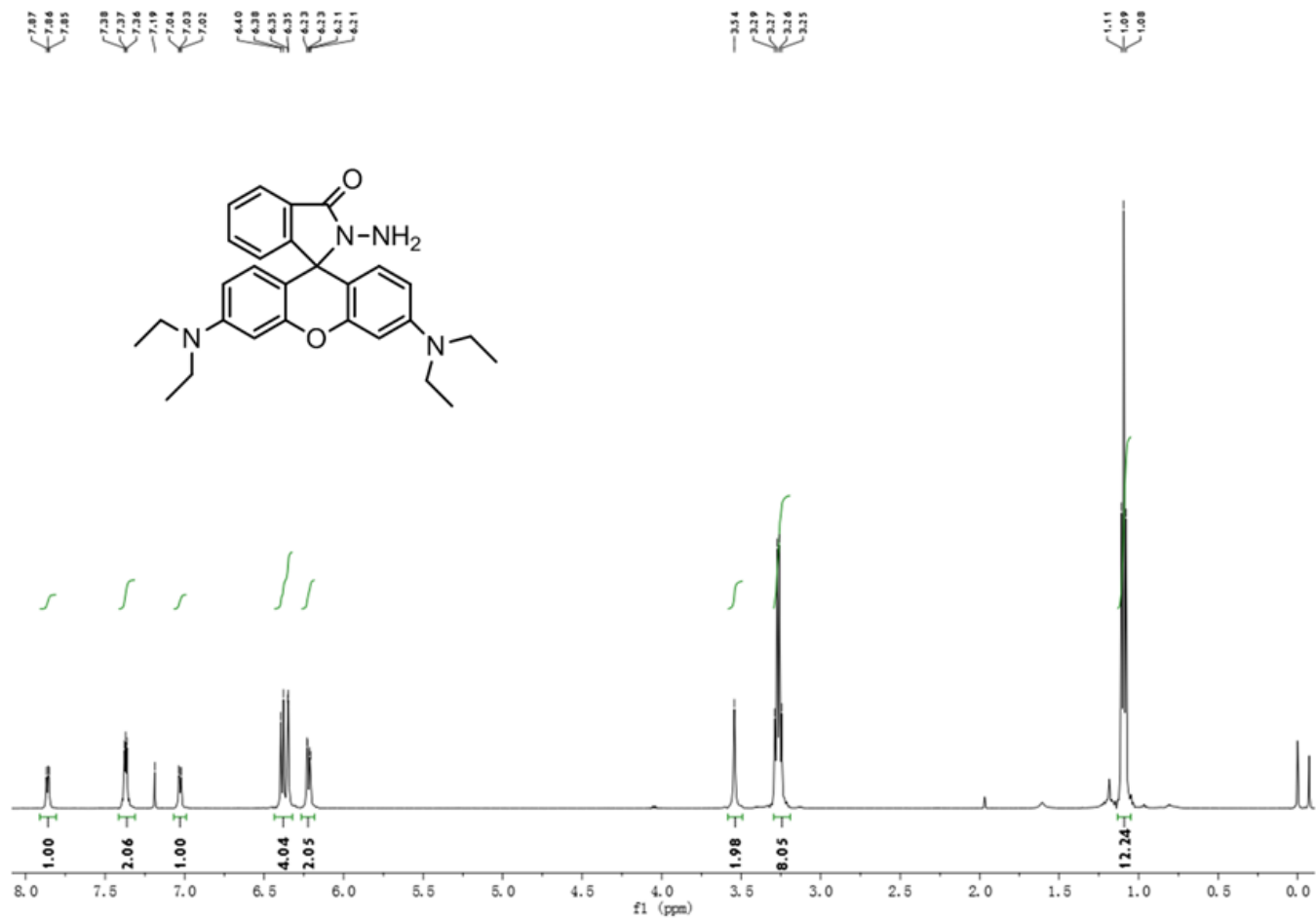


Figure S4. ¹H-NMR spectrum of Compound 1.

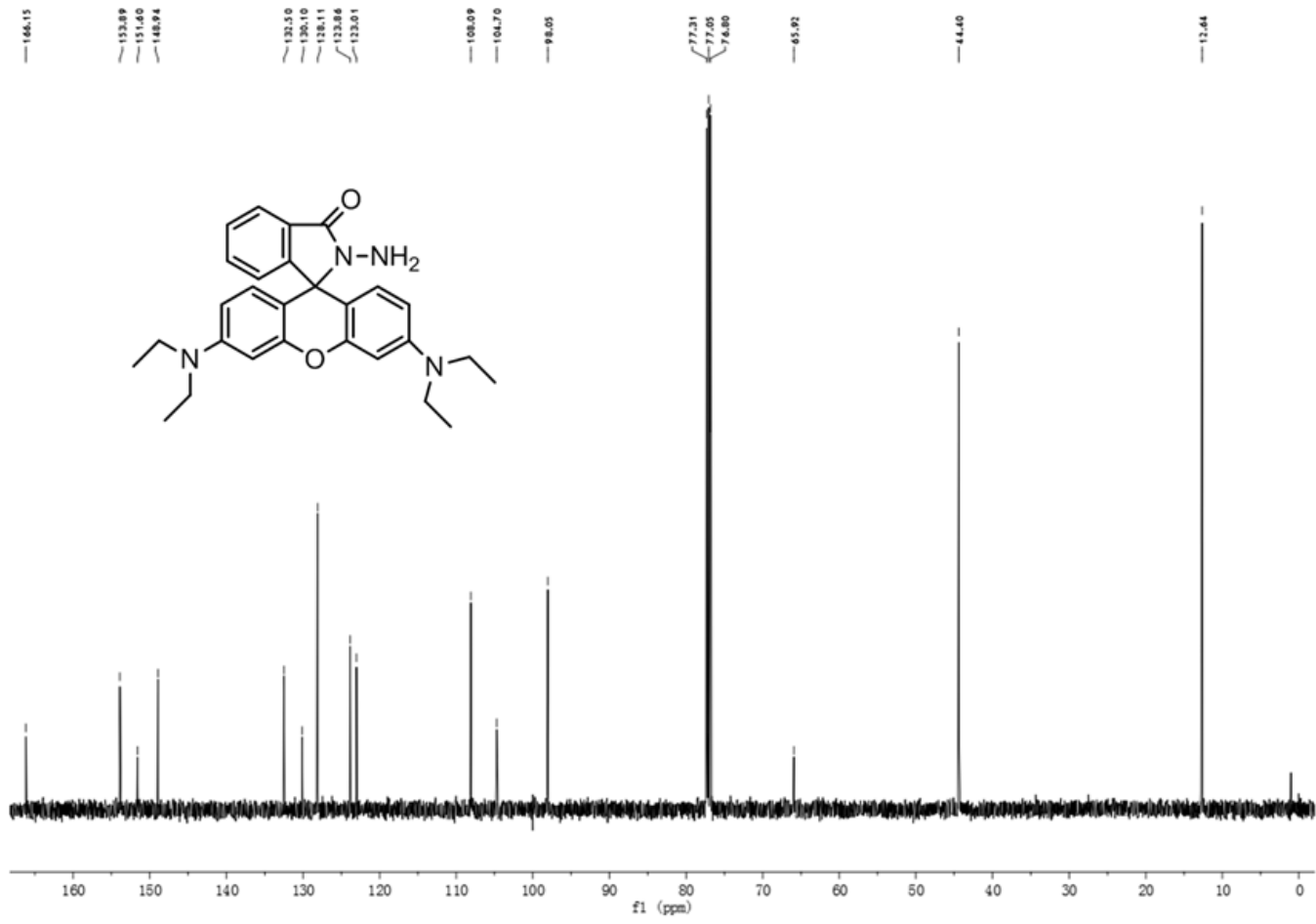


Figure S5. ^{13}C -NMR spectrum of Compound 1.

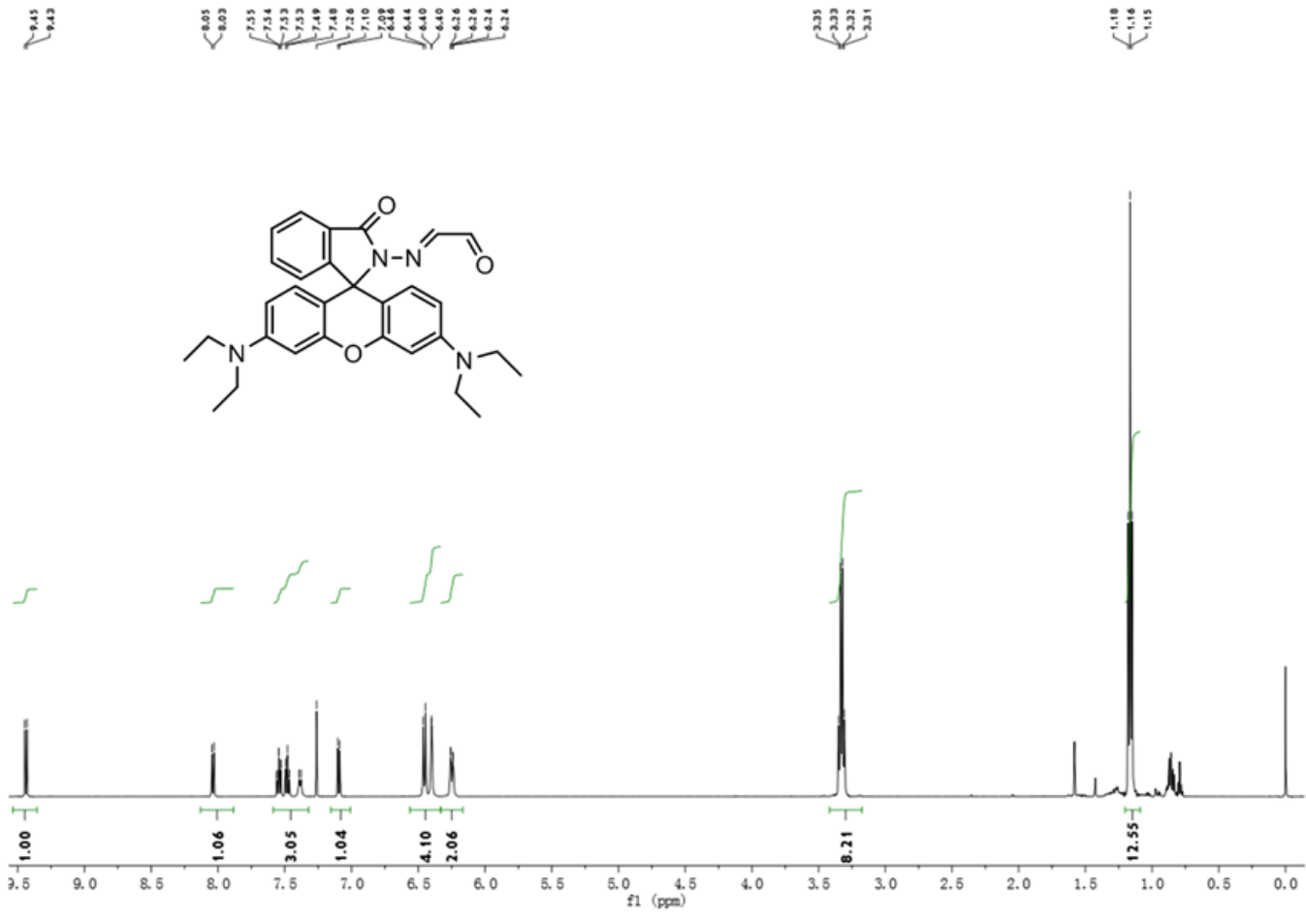


Figure S6. ¹H-NMR spectrum of Compound 2.

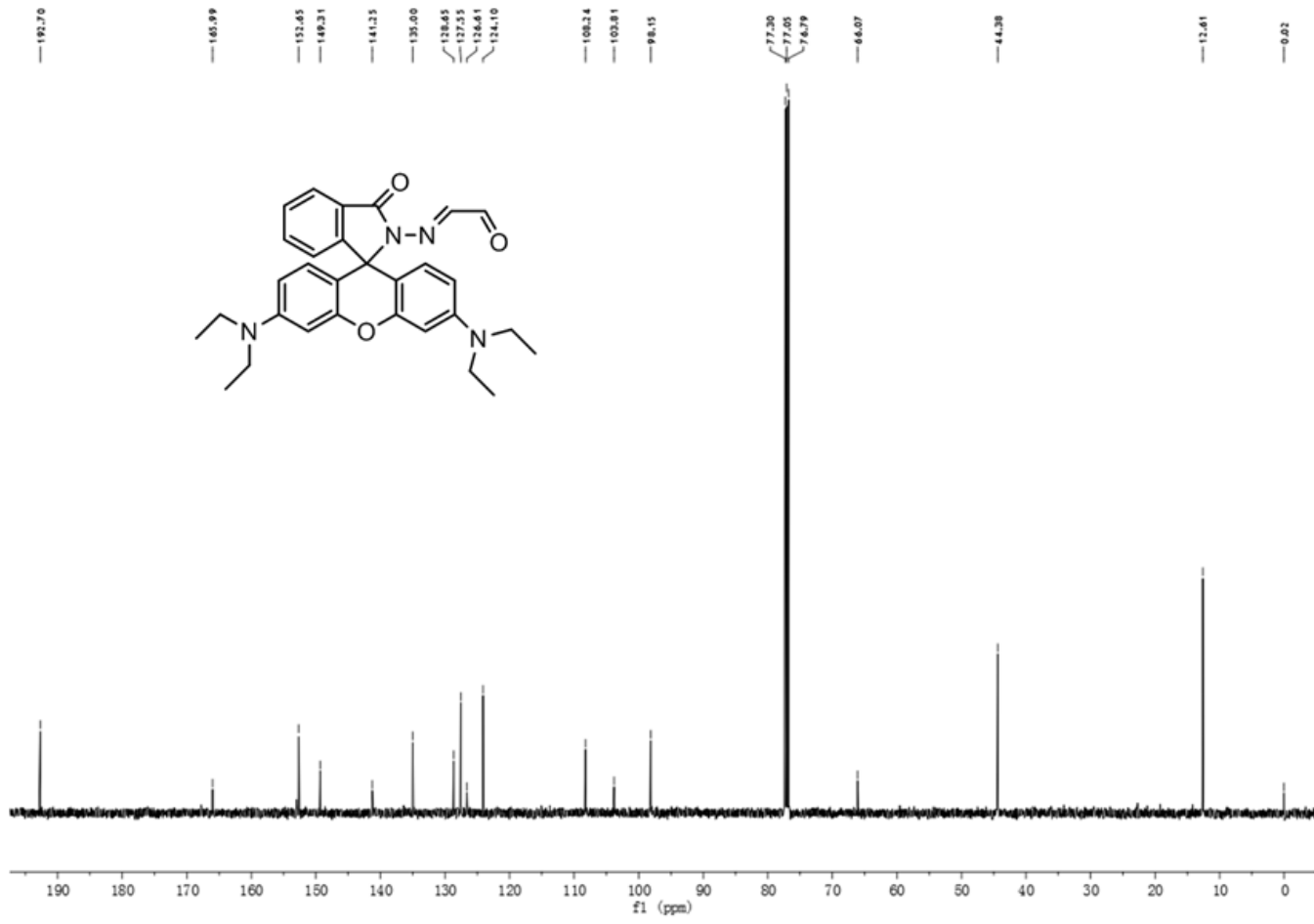


Figure S7. ^{13}C -NMR spectrum of Compound 2.

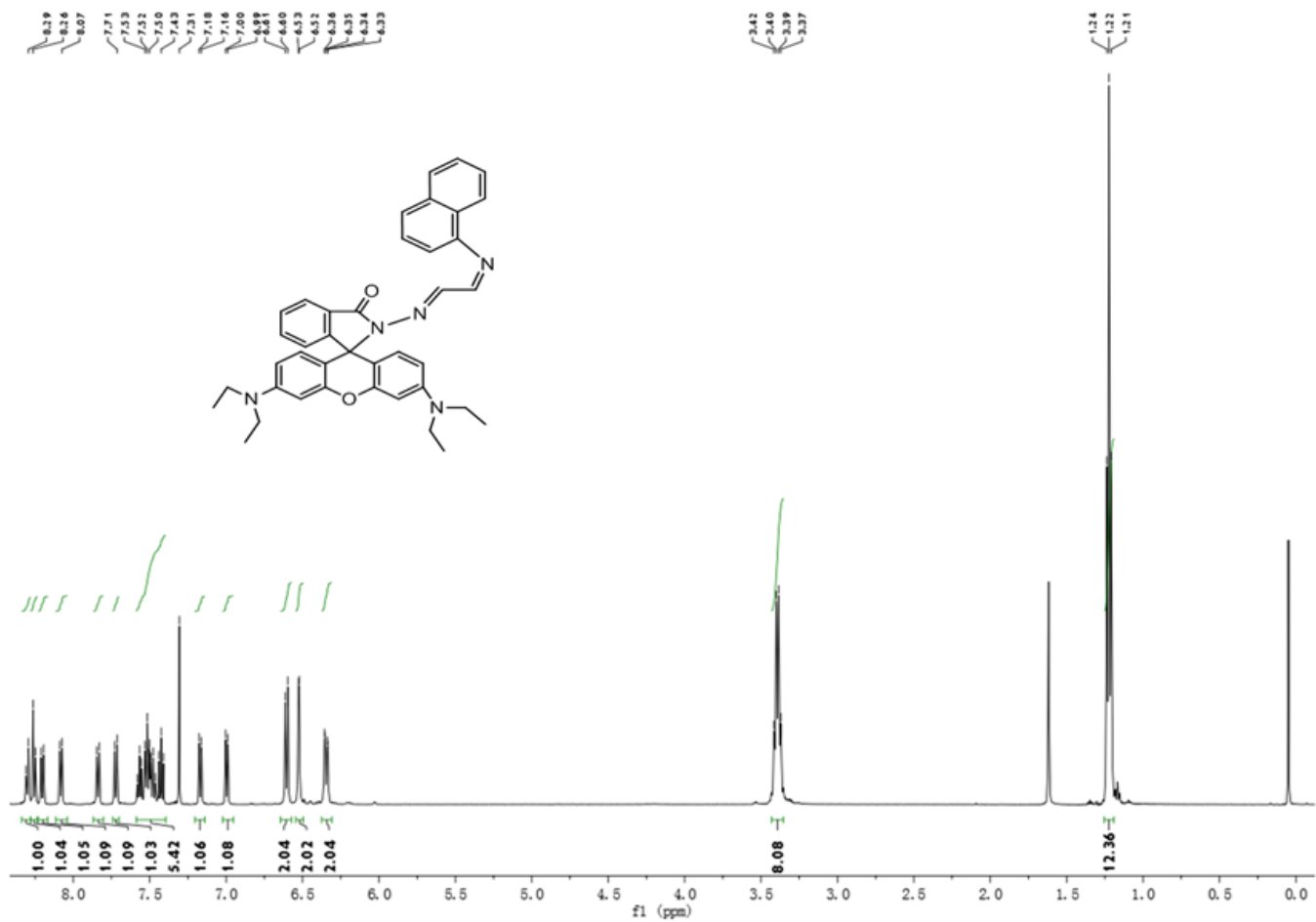


Figure S8. ^1H -NMR spectrum of RH-Fe.

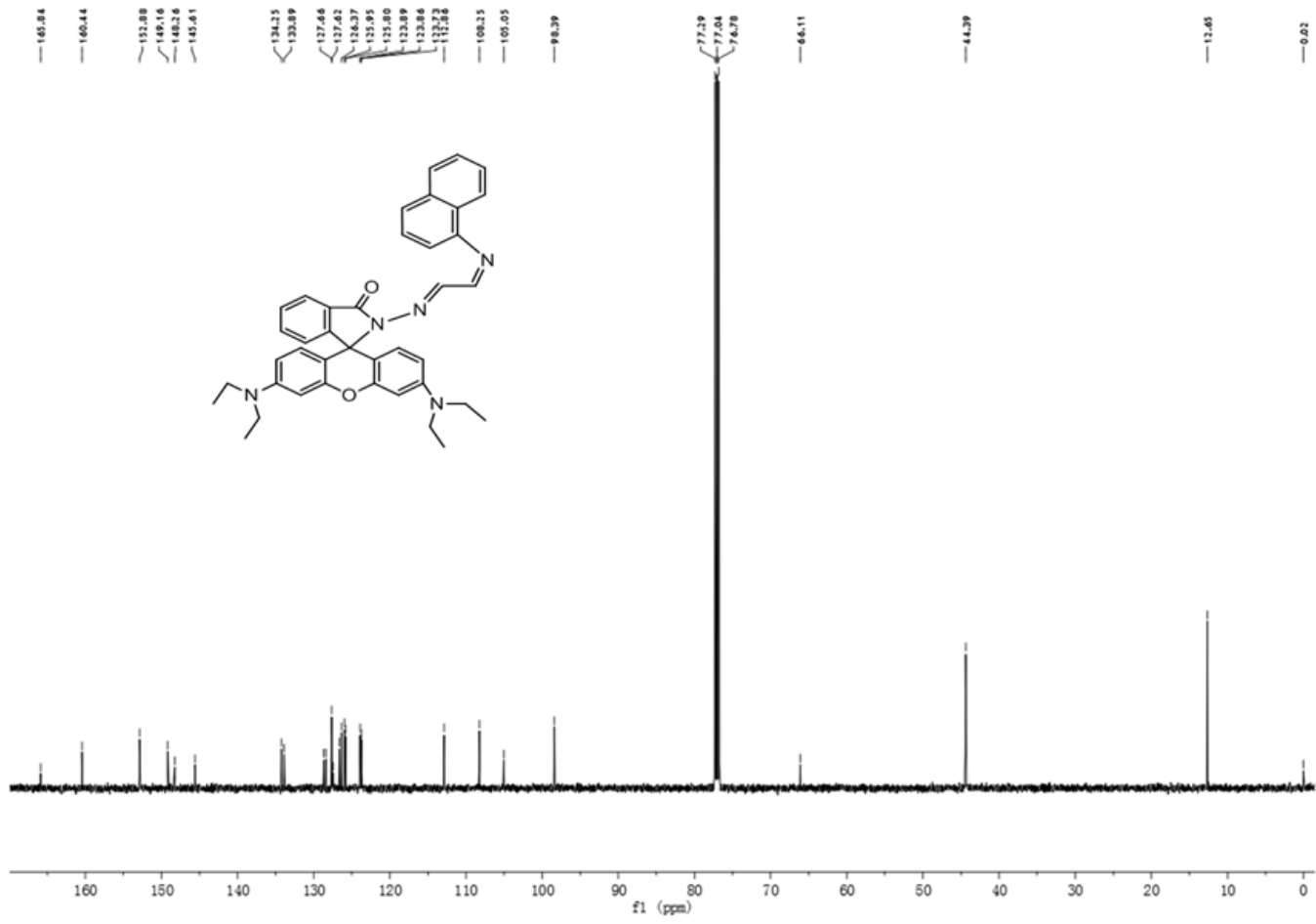


Figure S9. ^{13}C -NMR spectrum of RH-Fe.

[WJY]--HX1 #2-4 RT: 0.00-0.01 AV: 3 NL: 3.88E4
T: ITMS + c ESI sid=35.00 Full ms [50.00-2000.00]

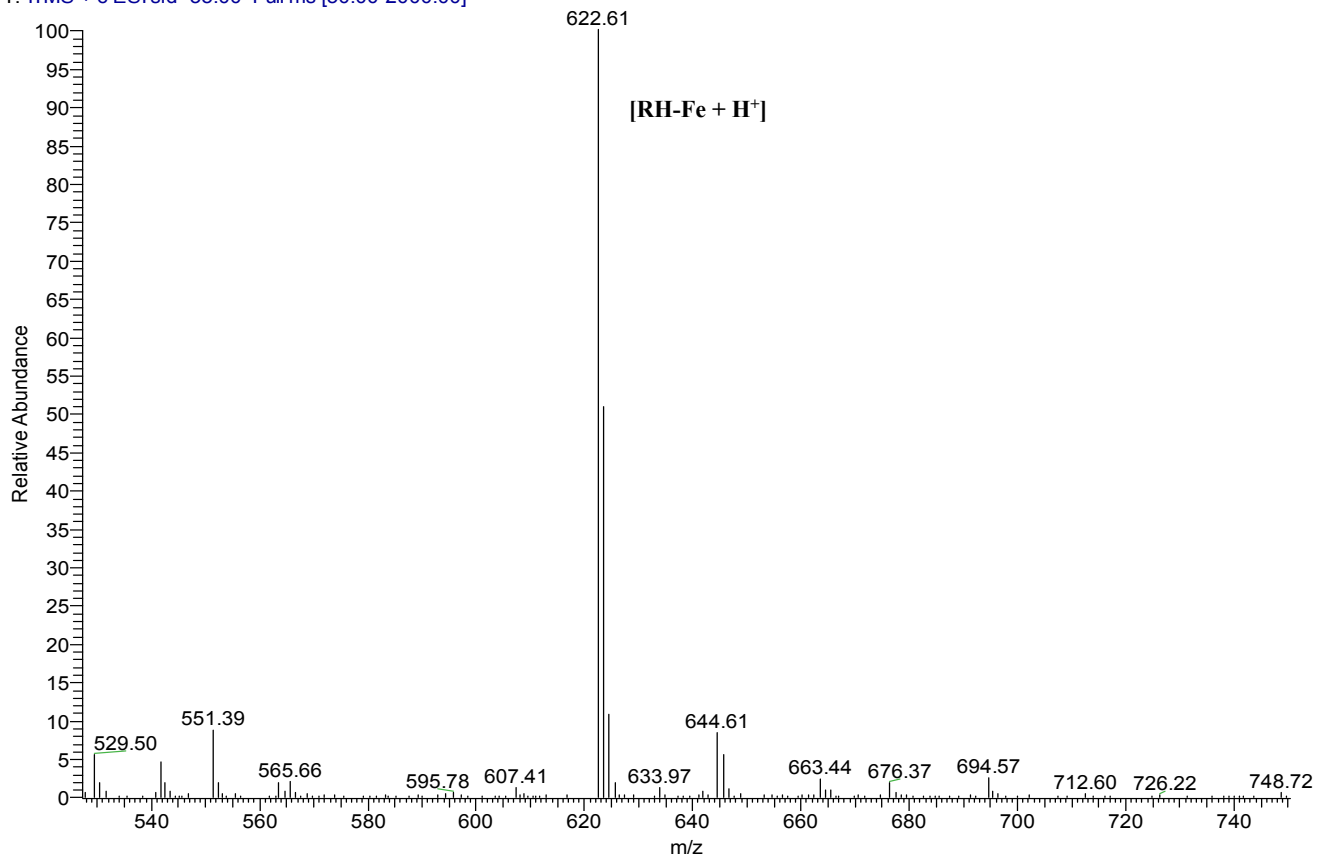


Figure S10. ESI-MS spectrum of RH-Fe.

[WJY]—HX-1 #54-61 RT: 0.73-0.82 AV: 8 NL: 4.45E2
T: ITMS + c ESI sid=35.00 Full ms [100.00-2000.00]

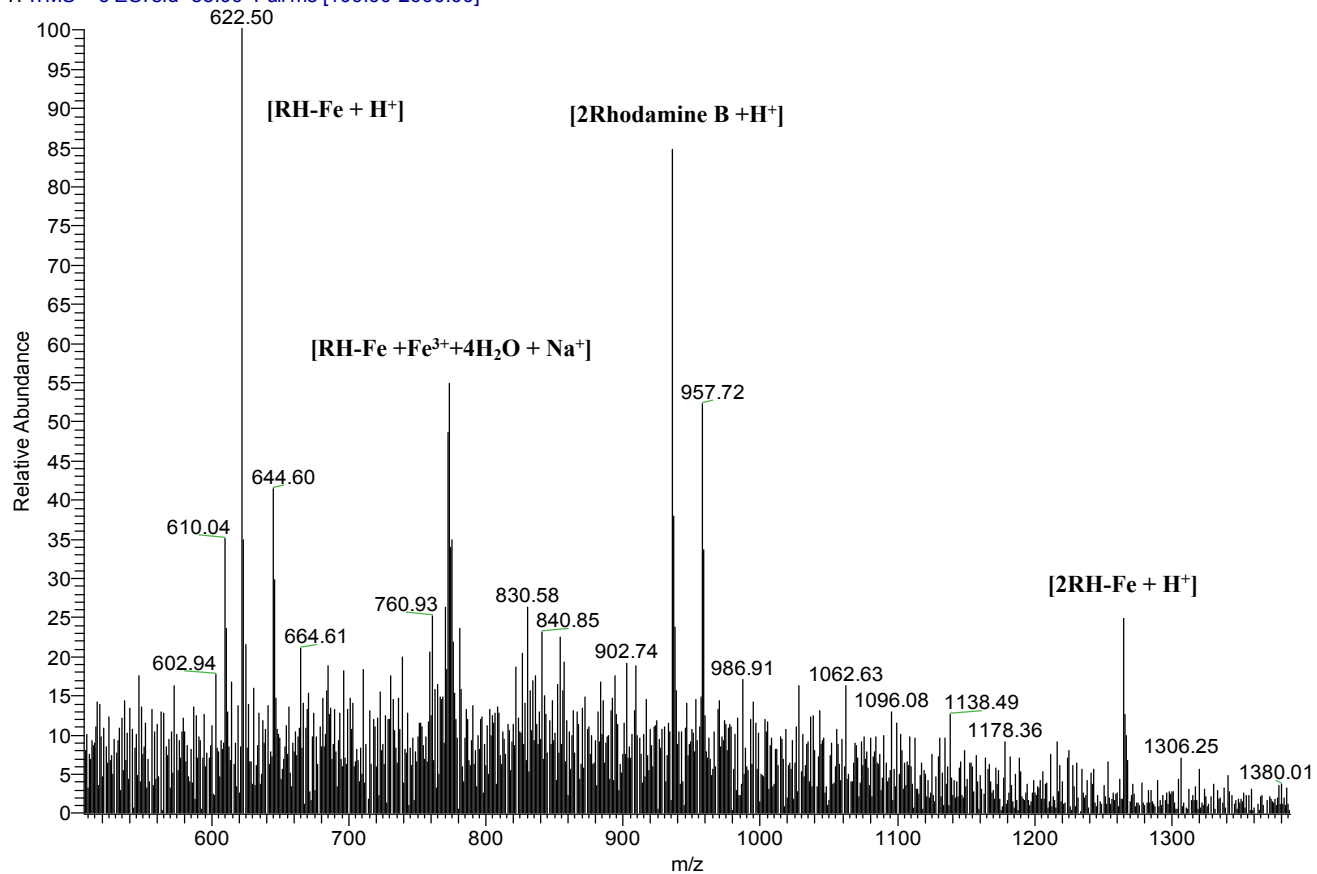


Figure S11. ESI-MS spectrum of RH-Fe in the presence of FeCl_3 .

S9. References for the Supplementary Information.

- [S1] X. B. Yang, B. X. Yang, J. F. Ge, Y. J. Xu, Q. F. Xu, J. Liang and J. M. Lu, *Org. Lett.*, 2011, **13**, 2710.
- [S2] X. X. Fang, S. F. Zhang, G. Y. Zhao, W. W. Zhang, J. W. Xu, A. M. Ren, C. Q. Wu and W. Yang, *Dyes Pigments*, 2014, **101**, 58.
- [S3] J. B. Li, Q. H. Hu, X. L. Yu, Y. Zhang, C. C. Cao, X. W. Liu, J. Guo and Z. Q. Pan, *J. Fluoresc.*, 2011, **21**, 2005.
- [S4] Y. Q. Liu, Z. H. Xu, J. H. Wang, D. Zhang, Y. Ye and Y. F. Zhao, *Luminescence*, 2014, **29**, 945.

- [S5] R. Kagit, M. Yildirim, O. Ozay, S. Yesilotand H. Ozay, *Inorg. Chem.*, 2014, **53**, 2144.
- [S6] U. Fegade, H. Sharma, S. Attarde, N. Singh and A. Kuwar, *J. Fluoresc.*, 2014, **24**, 27.
- [S7] K. Velmurugan, J. Prabhu, L. J. Tang, T. Chidambaram, M. Noel, S. Radhakrishnand and R. Nandhakumar, *Anal. Methods*, 2014, **6**, 2883.
- [S8] V. Luxami, Renukamal, K. Paul and S. Kumar, *RSC Adv.*, 2013, **3**, 9189.
- [S9] M. Y. She, Z. Yang, B. Yin, J. Zhang, J. Gua, W. T. Yin, J. L. Lia, G. F. Zhao and Z. Shi, *Dyes Pigments*, 2012, **92**, 1337.